Manuscripts, Articles, Book Chapters and Other Papers

12-15-2014

Cyclooxygenase-2, prostaglandin E2, and prostanoid receptor EP2 in fluid flow shear stress-mediated injury in the solitary kidney.

Tarak Srivastava
Children's Mercy Hospital

Uri S. Alon
Children's Mercy Hospital

Patricia A. Cudmore
Children's Mercy Hospital

Belal Tarakji
Children's Mercy Hospital

Alexander Kats
Children's Mercy Hospital

Let us know how access to this publication benefits you

See next page for additional authors

Follow this and additional works at: https://scholarlyexchange.childrensmercy.org/papers

Part of the Infectious Disease Commons, Nephrology Commons, Pathology Commons, Pediatrics Commons, and the Urogenital System Commons

Recommended Citation

Creator(s)

Tarak Srivastava, Uri S. Alon, Patricia A. Cudmore, Belal Tarakji, Alexander Kats, Robert E. Garola, R Scott Duncan, Ellen T. McCarthy, Ram Sharma, Mark L. Johnson, Lynda F. Bonewald, Ashraf El-Meanawy, Virginia J. Savin, and Mukut Sharma

CALL FOR PAPERS | *Novel Mechanisms and Roles of Glomerular Podocytes*

Cyclooxygenase-2, prostaglandin E_2, and prostanoid receptor EP2 in fluid flow shear stress-mediated injury in the solitary kidney

Tarak Srivastava,[1,5] Uri S. Alon,[1] Patricia A. Cudmore,[1] Belal Tarakji,[1] Alexander Kats,[2] Robert E. Garola,[2] R. Scott Duncan,[3] Ellen T. McCarthy,[4] Ram Sharma,[5] Mark L. Johnson,[6] Lynda F. Bonewald,[6] Ashraf El-Meanawy,[7] Virginia J. Savin,[4,5] and Mukut Sharma[4,5]

[1]*Section of Nephrology, Children's Mercy Hospital and University of Missouri-Kansas City, Kansas City, Missouri;*
[2]*Department of Pathology and Laboratory Medicine, Children's Mercy Hospital and University of Missouri-Kansas City, Kansas City, Missouri;* [3]*Section of Infectious Diseases, Children's Mercy Hospital and University of Missouri-Kansas City, Kansas City, Missouri;* [4]*Kidney Institute, University of Kansas Medical Center, Kansas City, Kansas;* [5]*Renal Research Laboratory, Research and Development, Kansas City Veterans Affairs Medical Center, Kansas City, Missouri;* [6]*Department of Oral Biology, University of Missouri-Kansas City School of Dentistry, Kansas City, Missouri; and* [7]*Division of Nephrology, Medical College of Wisconsin, Milwaukee, Wisconsin*

Srivastava T, Alon US, Cudmore PA, Tarakji B, Kats A, Garola RE, Duncan RS, McCarthy ET, Sharma R, Johnson ML, Bonewald LF, El-Meanawy A, Savin VJ, Sharma M. Cyclooxygenase-2, prostaglandin E_2, and prostanoid receptor EP2 in fluid flow shear stress-mediated injury in the solitary kidney. *Am J Physiol Renal Physiol* 307: F1323–F1333, 2014. First published September 18, 2014; doi:10.1152/ajprenal.00335.2014.—Hyperfiltration subjects podocytes to increased tensile stress and fluid flow shear stress (FFSS). We showed a 1.5- to 2.0-fold increase in FFSS in uninephrectomized animals and altered podocyte actin cytoskeleton and increased synthesis of prostaglandin E_2 (PGE_2) following in vitro application of FFSS. We hypothesized that increased FFSS mediates cellular changes through specific receptors of PGE_2. Presently, we studied the effect of FFSS on cultured podocytes and decapsulated isolated glomeruli in vitro, and on solitary kidney in uninephrectomized sv129 mice. In cultured podocytes, FFSS resulted in increased gene and protein expression of cyclooxygenase (COX)-2 but not COX-1, prostanoid receptor EP2 but not EP4, and increased synthesis and secretion of PGE_2, which were effectively blocked by indomethacin. Next, we developed a special flow chamber for applying FFSS to isolated glomeruli to determine its effect on an intact glomerular filtration barrier by measuring change in albumin permeability (P_{alb}) in vitro. FFSS caused an increase in P_{alb} that was blocked by indomethacin ($P < 0.001$). Finally, we show that unilateral nephrectomy in sv129 mice resulted in glomerular hypertrophy ($P = 0.006$), increased glomerular expression of COX-2 ($P < 0.001$) and EP2 ($P = 0.039$), and increased urinary albumin excretion ($P = 0.001$). Activation of the COX-2-PGE_2-EP2 axis appears to be a specific response to FFSS in podocytes and provides a mechanistic basis for alteration in podocyte structure and the glomerular filtration barrier, leading to albuminuria in hyperfiltration-mediated kidney injury. The COX-2-PGE_2-EP2 axis is a potential target for developing specific interventions to ameliorate the effects of hyperfiltration-mediated kidney injury in the progression of chronic kidney disease.

podocytes; fluid flow shear stress; glomerular hemodynamics; hyperfiltration; glomerular filtration barrier

Address for reprint requests and other correspondence: T. Srivastava, Section of Nephrology, Children's Mercy Hospital, 2401 Gillham Rd., Kansas City, MO 64108 (e-mail: tsrivastava@cmh.edu).

A NORMAL GLOMERULAR FILTRATION rate (GFR) is important for maintaining homeostasis. Adaptive changes in glomerular hemodynamics start even before metabolic and clinical signs of chronic kidney disease (CKD) begin to manifest. In children born with congenital anomalies of the kidney and urinary tract (CAKUT) including a solitary kidney, the decrease in functional nephron mass leads to adaptive hyperfiltration. Hyperfiltration involves increased renal blood flow, glomerular capillary pressure (P_{GC}), single-nephron GFR (SNGFR), filtration fraction, and decreased hydraulic conductivity associated with glomerular hypertrophy (4, 5). A considerable number of children born with a solitary kidney develop albuminuria during adolescence and progress to renal end-stage disease (ESRD) as young adults (34, 51–53). Investigating the interplay of mechanical forces on podocytes within the glomerulus may provide a better understanding of hyperfiltration-mediated kidney injury.

Podocytes are exposed to mechanical forces such as tensile stress as a result of capillary wall stretch and fluid flow shear stress (FFSS) due to the flow of the ultrafiltrate (11, 17, 40, 41). Glomerular capillary pressure creates tensile stress on the capillary wall, which leads to stretching of the podocyte foot processes that tightly cover the capillary. The tensile stress (or stretch) is exerted over the basolateral aspect of the podocyte from the stress in the vascular compartment that is studied in vitro using a biaxial elongation (or substrate stretch) model (11). The flow of glomerular ultrafiltrate creates shear stress on the surface of the podocyte and causes cellular deformation. FFSS, largely exerted over the exposed outer aspect of major processes and the soma of podocytes, is studied in vitro using a flow chamber (17, 41). Differences between the effects of these forces are not well understood, but FFSS appears to mediate greater change in cell morphology compared with stretch (27).

Previously, we showed that the calculated FFSS over podocytes is increased 1.5–2.0-fold in unilateral nephrectomy animal models (40). FFSS applied to podocytes in vitro resulted in an altered actin cytoskeleton, upregulation of cyclooxygenase (COX)-2, and increased secretion of PGE_2 (41). PGE_2 is known to modulate glomerular hemodynamics and permselectivity (26, 37). We hypothesized that a hyperfiltration-induced

increase in FFSS over podocytes increases PGE$_2$ synthesis, which alters the filtration barrier, leading to albuminuria, kidney injury, and progression of CKD. To investigate the role of COX-2 and PGE$_2$ in hyperfiltration-mediated kidney injury, we studied the effect of FFSS on *1*) cultured podocytes in vitro, *2*) isolated decapsulated rat glomeruli, and *3*) sv129 mice following unilateral nephrectomy. This report highlights the significance of the COX2-PGE$_2$-EP2 axis in podocytes exposed to FFSS. FFSS-mediated changes could be the mechanistic basis for albuminuria and progression of CKD in hyperfiltration-mediated kidney injury. We believe this COX-2-PGE$_2$-EP2 axis is a potential target for developing interventions to prevent CKD progression in CAKUT.

MATERIALS AND METHODS

Animals. Studies involving rats and mice were carried out using protocols approved by the Institutional Animal Care and Use Committee (IACUC), Safety Subcommittee, and the R&D Committee at the Veterans Affairs Medical Center (Kansas City, MO). Male Sprague-Dawley rats (7–8 wk old) from Harlan (Madison, WI) and male sv129 mice (13–14 wk) from Charles River (Indianapolis, IN) were obtained. Animals were maintained at Association for Assessment and Accreditation of Laboratory Animal Care-approved facilities with unrestricted access to food and water under 12:12-h light-dark cycles.

Cell culture. Conditionally immortalized mouse podocyte line (kind gift from Peter Mundel) with thermosensitive tsA58 mutant T antigen was used in these studies. Podocytes were propagated in RPMI 1640 with L-glutamine supplemented with 10% fetal bovine serum, 100 U/ml penicillin, and 0.1 mg/ml streptomycin (Invitrogen, Carlsbad, CA) under permissive conditions (33°C with 10 U/ml of γ-interferon, Cell Sciences, Norwood, MA). To induce differentiation, cells were transferred to nonpermissive conditions (37°C without γ-interferon). Three glass slides (25 × 75 × 1 mm, Fischer Scientific, Pittsburgh, PA) were maintained in one culture dish containing 12 ml of culture medium. Differentiated podocytes were used for FFSS experiments on *day 14*. We evaluated the podocyte actin cytoskeleton with phalloidin tagged to Alexa Fluor 568 and cell morphology by crystal violet stain as described earlier by us (41).

FFSS application to podocytes. FFSS was applied to differentiated podocytes using a FlexCell Streamer Gold apparatus (Flexcell, Hillsborough, NC). The apparatus was sterilized with 300 ml of 70% ethanol for 30 min and checked for leaks. This was followed by two wash steps with 300–400 ml of sterilized PBS for 5 min each. PBS was then replaced by 350 ml of media. The flow chamber was moved to a sterile hood by using sterilized forceps. One glass slide with podocytes was placed in each one of the slots of the flow device chamber. All six slots were filled to ensure consistent flow. The chamber was then placed in the incubator at 37°C with 5% CO$_2$. The computer was programmed to apply FFSS at 2 dynes/cm^2 (or 75 ml/min) for 2 h at 37°C with 5% CO$_2$. In another set of experiments, podocytes were incubated with indomethacin (2.5 μM, 1 h) before application of FFSS. Following FFSS treatment, podocytes on slides were returned to the original medium for recovery up to 24 h in the incubator at 37°C under a 5% CO$_2$ humidified atmosphere. In a set of experiments a three-way stop-cock was attached to collect 1.5 ml aliquots of the medium at 0, 30, and 120 min during application of FFSS. Control podocytes were grown on glass slides and placed in the same hood and incubator as experimental cells but were not exposed to FFSS. We evaluated the suitability of untreated "no-flow" control as a surrogate for very low FFSS under physiological conditions. Untreated cells were compared with podocytes exposed to low FFSS at 0.2 dynes/cm^2 for 2 h using the flow cell we developed to apply FFSS to glomeruli (see below). Samples obtained before FFSS and post-FFSS treatment were termed pre-FFSS, post-2hr and post-24hr, respectively. Culture media were collected from control podocytes at the same time points. Pre-FFSS and post-FFSS (2 h/24 h) cells were harvested for analysis.

Enzyme immunoassay to determine changes in secreted and intracellular PGE$_2$. PGE$_2$ in media and the cell lysate was measured using a PGE$_2$ EIA kit (514010, Cayman Chemical, Ann Arbor, MI) following the manufacturer's instructions.
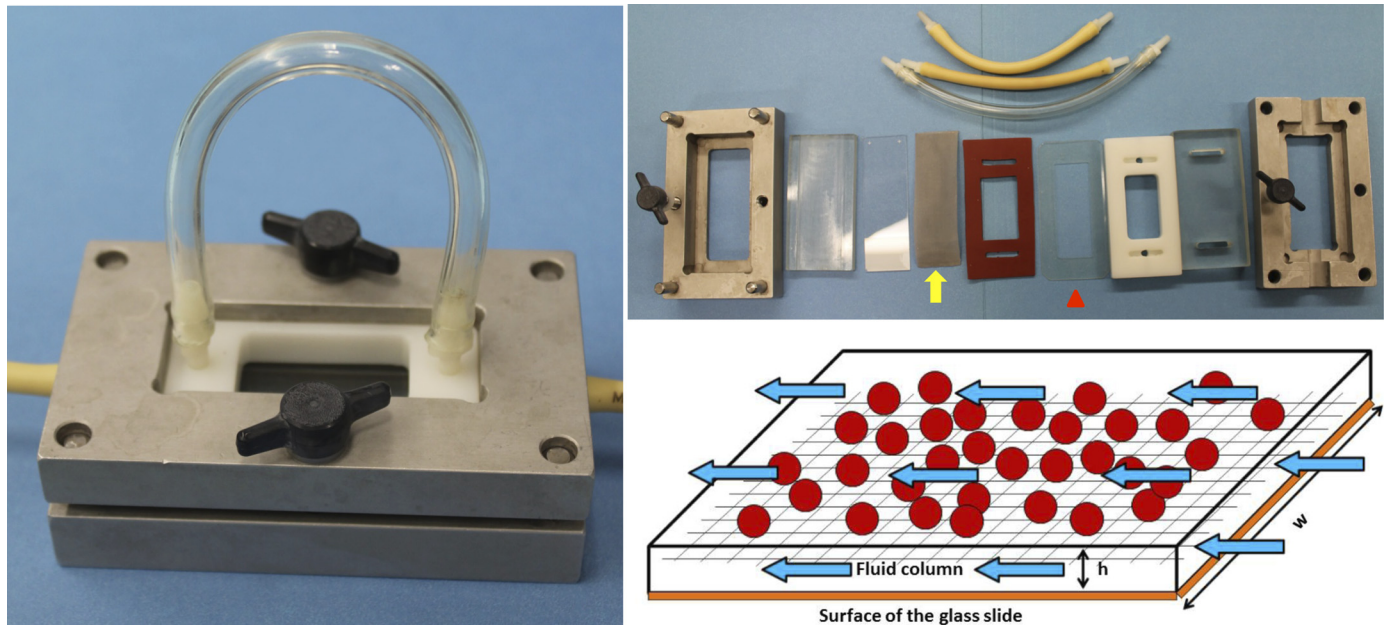

Fig. 1. Flow chamber for application of fluid flow shear stress (FFSS) over glomeruli. The flow chamber is constructed of metal, rubber, and plastic parts to allow laminar flow and to create a seal to prevent fluid leak. *Left*: flow chamber assembled for an experiment. *Top right*: lower and upper sides of the metal chamber, plexiglas base and top, glass slide, steel mesh, rubber gaskets, and plastic spacer. The thickness and the width of the plastic spacer (*top right*, red arrowhead) determine the height of the fluid column. *Bottom right*: schematic illustrating the line diagram for flow of the fluid column over the glomeruli kept in place by a mesh screen (yellow arrow, *top right*).

Quantitative real-time PCR to determine gene expression of cyclo-oxygenase enzymes and prostanoid receptors in podocytes. Podocyte total RNA was extracted using the Micro-Midi Total RNA Purification System (Invitrogen) and analyzed for quality and quantity by absorbance at 260 and 280 nm using a DNA/RNA calculator (Pharmacia Biotech/GE Healthcare, Uppsala, Sweden). The OD$_{260}$/OD$_{280}$ absorbance ratio was 1.8–2.0, indicating clean RNA preparations. One microgram of total RNA was reverse transcribed using the SuperScript III First Strand Synthesis System (Invitrogen). Quantitative real-time PCR (RT-qPCR) was performed with SYBR Supermix (Bio-Rad, Hercules, CA) using a Bio-Rad iCycler (Bio-Rad) with specific sets of primers for each of the COX enzymes, EP receptors, and β-actin. β-Actin was used as the housekeeping gene. Samples from five separate experiments were analyzed by RT-qPCR for each experimental condition, i.e., FFSS with or without indomethacin. The sequences (5′-3′) of primers used for RT-qPCR are shown in Table 5. PCR products were sequenced to further confirm the COX enzymes, EP receptors, and β-actin at the KUMC Core Facilities (Kansas City, KS).

Western blotting to determine protein expression of COX enzymes and prostanoid receptors in podocytes. Podocytes were lysed with RIPA buffer containing protease and phosphatase inhibitors. Total protein was determined using a bicinchoninic acid protein assay kit (BCA1, Sigma-Aldrich, St. Louis, MO). Western blotting was performed as described previously (42). Briefly, proteins were denatured in sample buffer containing β-mercaptoethanol at 94°C for 5 min. Ten micrograms of total protein was electrophoresed on a 10% Bis-Tris gel. Proteins were transferred to a polyvinylidene membrane, washed with PBST (0.1% Tween 20) and blocked using 5% nonfat milk. A rabbit polyclonal COX-1 antibody (sc-7950, Santa Cruz Biotechnol-

ogy, Dallas, TX) at 1:200 dilution, COX-2 antibody (ab6665, Abcam, Cambridge, MA) at 1:2,000 dilution, EP2 antibody (sc-20675, Santa Cruz) at 1:500 dilution, and EP4 antibody (ab93486, Abcam) at 1:2,000 dilution were used. After washing with PBST, the membrane was incubated with horseradish peroxidase-conjugated secondary antibody to each primary antibody. Chemiluminescence (ECL, GE Healthcare Biosciences, Piscataway, NJ) reagent was used for detection on X-ray film. Developed X-ray films were imaged and analyzed using FluorChem using built-in AlphaEaseFC software (Alpha Innotech, San Leandro, CA). Samples from three to five replicates for each experimental treatment (FFSS with or without indomethacin) were analyzed.

FFSS treatment of isolated rat glomeruli. Glomeruli were isolated as described below and placed on a stainless screen in a flow chamber designed and constructed in our laboratory. The flow chamber is constructed of a two-part metal shell to house a flow cell with fixed dimensions. The plexiglas base and top are lined with rubber gaskets to seal the glomeruli in a compartment with defined dimensions (Fig. 1). The thickness of the transparent plastic spacer determines the height of the fluid column. FFSS (τ; in dynes/cm^2) was calculated as τ = 6ηQ/(w * h^2), where η is viscosity, Q is rate of fluid flow, and w and h are width and height of the fluid column, respectively. FFSS was applied at 0.3 dyne/cm^2 for 60 or 120 min, and again following a recovery for 120 min at 37°C. In separate experiments, glomeruli were pretreated with 2.5 μmol/l indomethacin before FFSS treatment. Untreated glomeruli maintained in parallel without FFSS treatment were used as a control at time T_0 and T_{Final}. Glomeruli from four rats were used in separate experiments (20 glomeruli/group from $n = 4$ rats with 5 glomeruli/rat). Glomeruli from these treatment and control
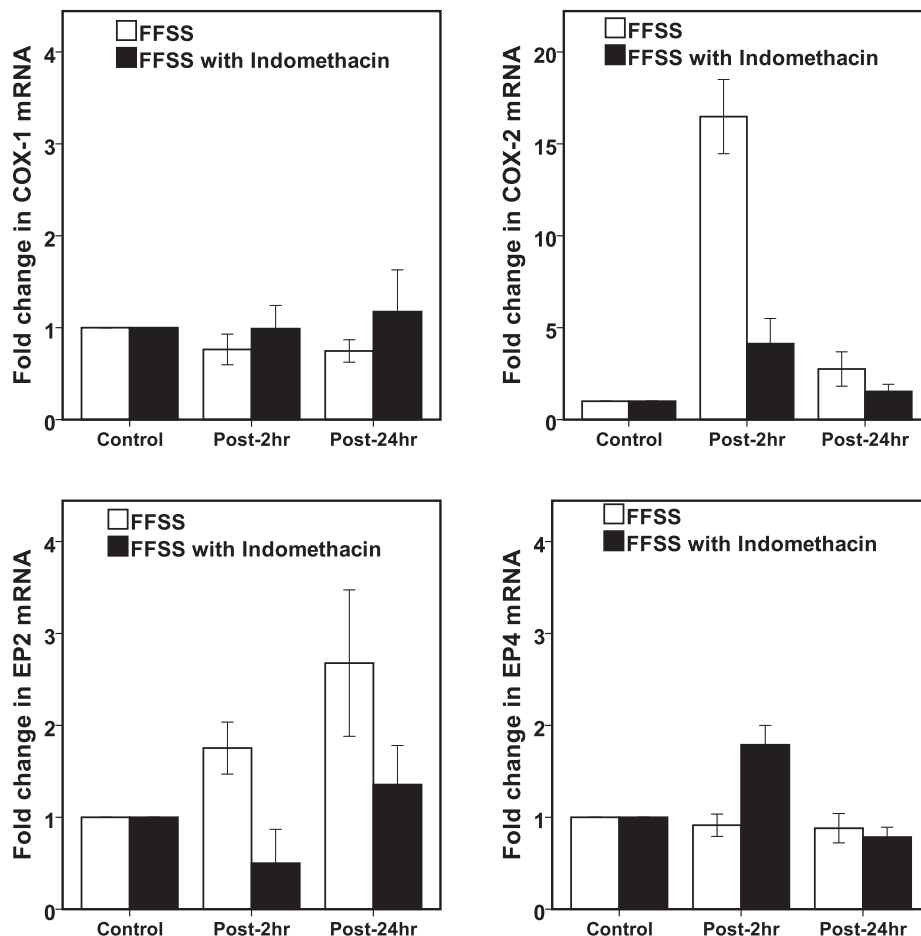

Fig. 2. FFSS induces cyclooxygenase (COX)-2 and EP2 gene expression. Cultured podocytes were exposed to FFSS at 2 dynes/cm^2 for 2 h with and without pretreatment with indomethacin. Control groups were maintained identically in the medium without FFSS. Total RNA was extracted from podocytes at 2 (post-2hr) and 24 h after FFSS (post-24hr). Total RNA was analyzed for COX-1, COX-2, EP2, and EP4 gene expression using real-time quantitative PCR (RT-qPCR). *Top*: FFSS resulted in increased COX-2 gene expression at post-2hr ($P < 0.001$ vs. control) that was attenuated by pretreatment with indomethacin. *Bottom*: FFSS resulted in increased EP2 gene expression at post-24hr ($P < 0.02$ vs. control) that was attenuated by pretreatment with indomethacin. Pretreatment with indomethacin caused a significant increase in EP4 gene expression at post-2hr ($P = 0.007$). Values are means ± SD of 5–6 replicate experiments. *$P < 0.05$.

groups were used to determine effect of FFSS on albumin permeability (P_{alb}) in vitro using the assay described

In vitro glomerular P_{alb} assay following FFSS. Control and FFSS-treated rat glomeruli were used to study the changes in glomerular filtration barrier characteristics using an in vitro assay established in our laboratory. Details of the assay to measure volume response of glomerular capillaries to an oncotic gradient generated by defined concentrations of albumin have been described previously (35, 38). Briefly, kidneys were removed from anesthetized male Sprague-Dawley rats (200–250 g) and decapsulated. The renal cortex was cut into fine fragments and consecutively passed through 80- and 120-mesh stainless screens. Glomeruli were recovered from atop the 200-mesh screen. Glomeruli were isolated at room temperature in a physiological buffer solution (pH 7.4). BSA (5 g/dl) was included in the medium as an oncotic agent (isolation/incubation buffer). Oncotic gradient was induced by changing BSA concentration in the bath medium to 1%. Oncotic pressure was measured using a membrane colloid osmometer (model 4100, Wescor, Logan, UT).

Following experimental treatments, glomeruli were incubated in 5% BSA medium for 15 min at 37°C, transferred to glass coverslips coated with poly-L-lysine, and observed using video microscopy. Measurements of glomerular volume were made before and 1 min after the initial incubation medium containing 5 gm/dl BSA was replaced by medium containing 1 g/dl BSA. Change of the medium produces an oncotic gradient across the glomerular capillary wall (5 g/dl BSA in the lumen vs. 1 g/dl BSA in the bathing medium) and results in net fluid influx and an increase in glomerular volume. Glomerular volume was calculated from the average of four diameters of the video image and the change in volume (ΔV) of each glomerulus in response to the oncotic gradient: $\Delta V = (V_{final} - V_{initial})/V_{initial} \times 100\%$. The increase in glomerular volume (ΔV) is directly related to the oncotic gradient ($\Delta \Pi$) applied across the capillary wall. We use this principle to calculate the reflection coefficient (σ_{alb}) using the ratio of ΔV of experimental to ΔV of control glomeruli in response to identical oncotic gradients: $\sigma_{alb} = \Delta V_{experimental}/\Delta V_{control}$. Convectional P_{alb} is defined as $(1 - \sigma_{alb})$ and describes the movement of albumin consequent to water flow on a unitless scale of 0 to 1. When σ_{alb} is zero, albumin moves at the same rate as water and P_{alb} is 1.0. When σ_{alb} is 1.0, albumin cannot cross the membrane with water and P_{alb} is zero.

Unilateral nephrectomy in sv129 mice. Five 13- to 14-wk-old sv129 mice underwent surgical removal of the right kidney. Another set of five 13- to 14-wk-old sv129 mice underwent a sham operation for experimental control. Four weeks later, the left kidney was harvested from all animals for analysis. The day before harvesting of kidneys, urine was collected for urine albumin and creatinine measurement. Urine albumin and creatinine were measured at the Mouse Metabolic Phenotyping Center, Vanderbilt University Medical Center (Nashville, TN). Kidneys were fixed in 10% formalin, embedded in paraffin, sectioned at 3–5 μm, and stained using Jones silver stain. Images were obtained using an Olympus BX60 (Hamburg, Germany) for light microscopy, and morphological measurements were made using computerized image-analysis software (Analysis) as described earlier (40, 41).

Immunohistochemistry to determine expression of COX enzymes and prostanoid receptors in sv129 mouse kidneys. Immunohistochemistry for COX and EP proteins was performed as described earlier (42). Primary antibodies used included a rabbit polyclonal COX-1 antibody (sc-7950, Santa Cruz Biotechnology, Dallas, TX) at 1:100 dilution, COX-2 antibody (ab6665, Abcam) at 1:150 dilution, EP2 antibody (sc-20675, Santa Cruz Biotechnology) at 1:25 dilution, and EP4 antibody (ab93486, Abcam) at 1:100 dilution. Tissue sections were mounted in 9:1 (glycerol:PBS) + 5% *N*-propyl gallate, and photomicrographed as described. We performed image analysis using the National Institutes of Health Image J software suite by quantifying the mean integrated density (average grey value × area) of 3,3-diaminobenzidine (DAB) staining within the glomerulus for COX and

EP proteins to obtain the net protein expression/glomerulus. Endothelial cells are localized on the intraluminal aspect of the glomerular capillary, while podocytes surround and cover the extraluminal aspect of the capillary wall. We also performed additional semiquantitative analysis using a scale of 0–4. Each glomerulus examined was assigned a score based upon the percentage of total podocytes that showed positive staining (above background to brown-black); 0 (no staining), 1 (<10% of podocytes), 2 (10–25% of podocytes), 3 (25–50% of podocytes), or 4 (>50% of podocytes staining).

Statistics. Data were analyzed with repeated measures ANOVA analyses for three-group comparisons and Student's *t*-test for two-group comparisons using SPSS 20 statistical software. A *P* value <0.05 was considered significant.

RESULTS

FFSS increases gene expression of COX-2, but not COX-1, in podocytes. Figure 2 (*top*) shows results of RT-PCR (RT-qPCR) quantification of COX-1 and COX-2 gene expression at 2 (post-2hr) or 24 h (post-24hr) after FFSS with or without pretreatment with indomethacin. COX-2 gene fold-expression increased significantly at post-2hr (15.7 ± 3.9, *P* < 0.001) and returned to near control levels by post-24hr (2.7 ± 1.6, *P* = 0.51). Indomethacin markedly attenuated the effect of FFSS, and the fold-increase in COX-2 gene expression was only 4.1 ± 2.7, *P* = 0.06 at post-2hr that returned to the control level (1.5 ± 0.8, *P* = 0.89) at post-24hr. In contrast, FFSS did not alter COX-1 expression (Fig. 2, *top*).

FFSS increases protein expression of COX-2, but not COX-1, in podocytes. Figure 3 shows results of Western blotting using antibodies to detect COX-1 and COX-2 proteins at post-2hr and post-24hr after FFSS with or without pretreatment with indomethacin. As with gene expression, on density analysis protein expression of COX-2/β-actin compared with control (2.67 ± 1.37) was increase at post-2hr (4.56 ± 0.55, *P* = 0.035) and post-24hr (4.06 ± 1.16, *P* = 0.10) and is shown as a fold-change in Fig. 3. Indomethacin attenuated the
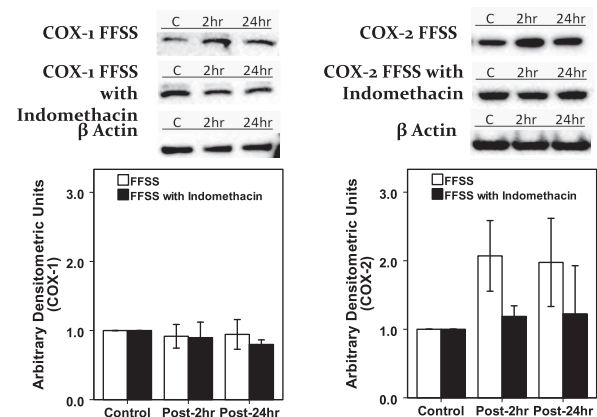

Fig. 3. FFSS upregulates COX-2 protein expression. Cultured podocytes were exposed to FFSS at 2 dynes/cm^2 for 2 h with and without pretreatment with indomethacin. Control groups were maintained identically in the medium without FFSS. Total protein lysates at post-2hr or post-24hr were analyzed by SDS-PAGE and Western blotting. β-Actin was used as the loading control to normalize density measurements. Bar graphs show fold-change (experimental/control) in density ratios (protein/β-actin). *Top*: images of representative immunoblots. *Left*: FFSS did not alter COX-1 protein expression. *Right*: FFSS resulted in increased COX-2 protein expression at 2hr post-FFSS (*P* = 0.035 vs. control) which was attenuated by indomethacin. COX-2 protein at post-24hr FFSS was not different from the control group. Values are means ± SD of 3–5 replicate experiments. **P* < 0.05.
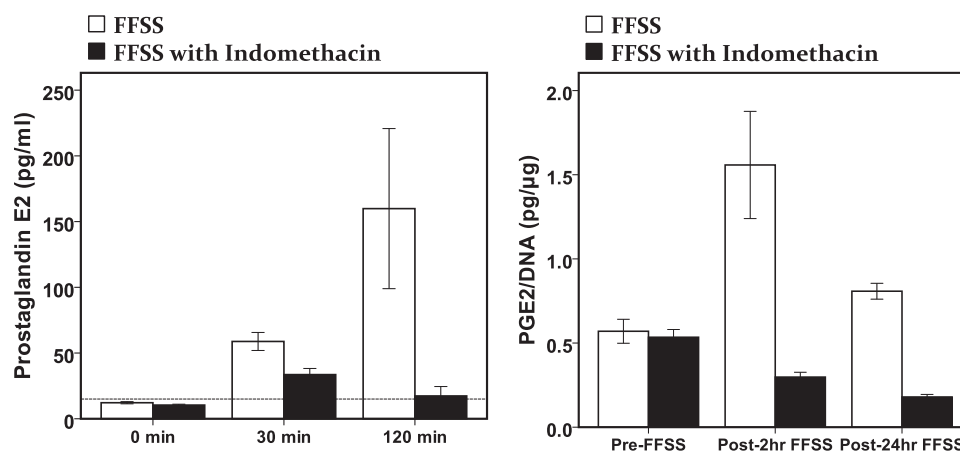
Fig. 4. FFSS increases secreted and intracellular PGE$_2$. Cultured podocytes were exposed to FFSS at 2 dynes/cm^2 for 2 h with and without pretreatment with indomethacin. The ELISA method was used to determine levels of PGE$_2$ in samples from 5–6 replicate experiments. Values are means $\pm$ SD. *Left*: PGE$_2$ levels (pg/ml) were elevated in aliquots of the medium collected at 30 and 120 min ($P = 0.04$) during FFSS application. The FFSS-induced increase in the levels of secreted PGE$_2$ was attenuated by indomethacin. *Right*: intracellular PGE$_2$ was normalized using DNA in each sample and expressed as PGE$_2$/DNA (pg/μg). FFSS caused an increase in the PGE$_2$/DNA ratio at post-2hr ($P = 0.02$ vs. control) and post-24hr ($P = $ NS vs. control) following FFSS. Pretreatment with indomethacin caused a decrease in intracellular PGE$_2$ at post-2hr ($P = 0.001$ vs. control) and post-24hr ($P = 0.001$ vs. control). *$P < 0.05$.

increase in COX-2. COX-1 protein expression did not change following FFSS with or without indomethacin.

FFSS stimulates PGE$_2$ synthesis in podocytes. Figure 4 shows the enzyme immunoassay results on the levels of PGE$_2$ in the medium at the onset (0 min), during FFSS (30 min), and at the end of FFSS (120 min) and the effect of FFSS on podocytes pretreated with indomethacin. PGE$_2$ was not detectable in the medium before applying FFSS (<15 pg/ml). FFSS caused an increase in PGE$_2$ levels in the medium by 30 (63.2 $\pm$ 13.6, $P = 0.57$) and 120 min (179.0 $\pm$ 149.1, $P = 0.04$). However, FFSS application for 30 or 120 min following pretreatment with indomethacin attenuated the increase in PGE$_2$ at 30 (33.6 $\pm$ 11.4, $P = 0.03$) and 120 min (17.4 $\pm$ 17.5, $P = 0.81$) (Fig. 4, *left*).

Figure 4 also shows that FFSS caused an approximately threefold increase in intracellular PGE$_2$. Pre-FFSS levels were 0.57 $\pm$ 0.16 pg PGE$_2$/μg DNA and post-2hr (1.56 $\pm$ 0.71 pg PGE$_2$/μg DNA, $P = 0.02$). Intracellular PGE$_2$ levels returned close to baseline by post-24hr FFSS (0.81 $\pm$ 0.11 pg PGE$_2$/μg DNA, $P = 0.69$). In contrast, pretreatment of podocytes with indomethacin caused a significant ($P = 0.001$) decrease in intracellular PGE$_2$ (control 0.53 $\pm$ 0.11, post-2hr 0.30 $\pm$ 0.07 and post-24hr 0.18 $\pm$ 0.03 pg PGE$_2$/μg DNA) (Fig. 4, *right*).

Table 1 summarizes the pattern of PGE$_2$ secretion up to 24 h after cessation of FFSS. PGE$_2$ levels were determined using ELISA in aliquots of medium collected at 2 and 24 h following FFSS treatment. FFSS caused a significant increase in PGE$_2$ concentration at post-2hr and post-24hr compared with control (Table 1). Pretreatment with indomethacin followed by FFSS blocked the increase in PGE$_2$ at both time points (Table 1).

FFSS increases gene expression of prostanoid receptor EP2 but not EP4. PGE$_2$ mediates its effect through four prostanoid receptors, EP1–EP4. Podocytes express EP1, EP2, and EP4 but not EP3 (42). Figure 2 (*bottom*) shows results of RT-qPCR measuring the gene expression of EP2 and EP4 at 2 (post-2hr) and 24 h (post-24hr) following FFSS with or without indomethacin pretreatment. FFSS significantly increased the gene expression of the EP2 receptor by post-24hr (2.7 $\pm$ 1.4, $P = 0.02$) but not at post-2hr (1.7 $\pm$ 0.5, $P = 0.4$). However, indomethacin did not alter EP2 gene expression significantly (post-2hr 0.5 $\pm$ 0.7, $P = 0.55$; post-24hr 1.4 $\pm$ 0.9, $P = 0.73$). In contrast, as shown in Fig. 2 (*bottom*), FFSS did not affect EP4 expression (post-2hr was 0.9 $\pm$ 0.2, $P = 0.86$; post-24hr 0.9 $\pm$ 0.3, $P = 0.76$). Interestingly, indomethacin caused a significant increase in EP4 gene expression at post-2hr 1.8 $\pm$ 0.4 ($P = 0.007$) but not at post-24hr 0.8 $\pm$ 0.2 ($P = 0.53$) following FFSS (Fig. 2, Lower panel).

FFSS increases protein expression of prostanoid receptor EP2 but not EP4. Figure 5 shows the effect of FFSS on podocyte EP2 and EP4 protein expression at post-2hr or

Table 1. *FFSS results in persistently elevated levels of secreted PGE$_2$*

| | PGE$_2$ in Supernatant Medium During Recovery Period After FFSS | | | | | |
| | FFSS without indomethacin | | | FFSS with indomethacin | | |
	Control	Experimental	P	Control	Experimental	P
Pre-FFSS	3,911 $\pm$ 1,567	4,847 $\pm$ 2,361	0.48	3,589 $\pm$ 2,002	4,077 $\pm$ 1,284	0.63
Post-2-h FFSS	3,767 $\pm$ 1,056	6,340 $\pm$ 2,078	0.04	3,450 $\pm$ 1,565	3,248 $\pm$ 1,010	0.79
Post-24-h FFSS	2,756 $\pm$ 820	6,980 $\pm$ 2,606	0.01	2,606 $\pm$ 1,121	2,313 $\pm$ 851	0.22

Values are means $\pm$ SD; $n = 5$–6 replicate experiments. Cultured podocytes were exposed to fluid flow shear stress (FFSS) at 2 dynes/cm^2 for 2 h with and without pretreatment with indomethacin. Control podocytes were maintained identically in the medium without FFSS. PGE$_2$ in the medium (pg) from podocytes exposed to FFSS was measured before FFSS and during recovery at post-2 h and post-24 h after FFSS. Control consisted of aliquots obtained from culture medium of untreated podocytes (i.e., no FFSS) at the same time points. PGE$_2$ levels in the medium at post-2-h and post-24-h time points were significantly increased compared with control in podocytes after FFSS, which were attenuated by pretreatment with indomethacin.
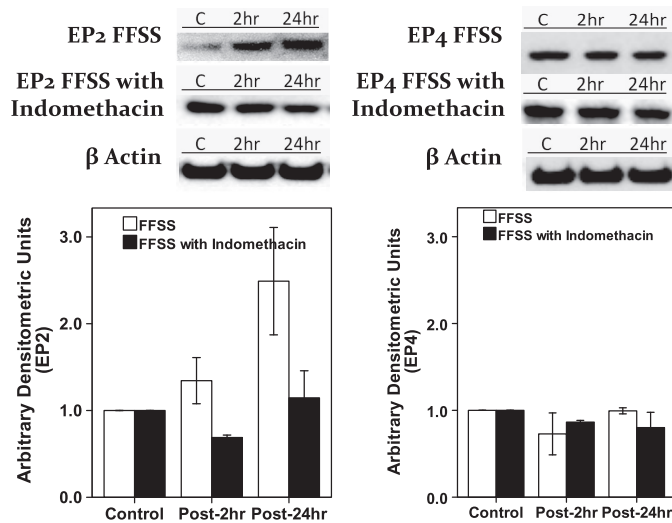
Fig. 5. FFSS increases protein expression of prostanoid receptor EP2. Cultured podocytes were exposed to FFSS at 2 dynes/cm^2 for 2 h with and without pretreatment with indomethacin. Control groups were maintained identically in the medium without FFSS. Total protein lysates at post-2hr or post-24hr were analyzed by SDS-PAGE and Western blotting. β-Actin was used as the loading control to normalize density measurements. Bar graphs show fold-change (experimental/control) in density ratios (protein/β-actin). *Top*: images of representative immunoblots. *Left*: FFSS resulted in increased EP2 expression at post-2hr ($P = 0.72$) and post-24hr (0.06) that was blocked by indomethacin. *Right*: FFSS did not alter the expression of EP4 protein. Values are means ± SD of 3–5 replicate experiments. *$P < 0.05$.

post-24hr using Western blotting. FFSS caused a gradual change in the (EP2/β-actin) density that increased from (0.29 ± 0.12, $P = 0.72$) at post-2hr to (0.50 ± 0.13, $P = 0.06$) by post-24hr compared with control (0.25 ± 0.16) and is shown as a fold-change in Fig. 5. Indomethacin attenuated the effect of FFSS on EP2 protein expression. However, FFSS, with or without indomethacin, did not alter the expression of EP4 protein.

Thus an FFSS stimulus to cultured podocytes increased the synthesis and secretion of PGE$_2$ into the extracellular milieu and upregulated the expression of the EP2 receptor, but not of EP4. An ~30% increase in secreted PGE$_2$ by post-2hr and only an ~10% increase between 2 and 24 h post-FFSS suggest a parallel rise in PGE$_2$ secretion and COX-2 expression (Table 1 and Fig. 3). Indomethacin effectively attenuated the changes induced by FFSS.

Control podocytes with no flow vs. low FFSS at 0.2 dynes/cm. Podocytes did not show a qualitative change in cell morphology or the actin cytoskeleton at post-2hr and post-24hr treated with low FFSS at 0.2 dynes/cm^2 for 2 h compared with the no-flow control ($n = 3$). In contrast, we have shown that FFSS at 2 dynes/cm^2 for 2 h causes significant changes in cell morphology and the actin cytoskeleton (41). FFSS at 0.2 dynes/cm^2 on podocytes did not increase the secreted PGE$_2$. PGE$_2$ levels in the medium at 30 and 120 min during FFSS were below the detection limit. Intracellular PGE$_2$ at post-2hr FFSS at 0.2 dynes/cm^2 (0.79 ± 0.20 pg/µg DNA) did not increase compared with the no-flow control (0.71 ± 0.14, $P = 0.56$). In contrast, both secreted and intracellular PGE$_2$ levels were increased after application of FFSS at 2 dynes/cm^2 for 2 h (Fig. 4, Table 1). Thus the no-flow control used in our studies

and low FFSS at 0.2 dynes/cm^2 approximating physiological conditions did not alter cellular structure or PGE$_2$ production.

Ex vivo application of FFSS to isolated decapsulated glomeruli results in increased P_{alb}. Previously, we showed that the PGE$_2$-induced increase in P_{alb} was blocked by indomethacin (26). Following the observation that application of FFSS increases PGE$_2$ in podocytes (Fig. 4), we determined the effect of FFSS on P_{alb} in isolated decapsulated rat glomeruli.

Table 2 and Fig. 6 summarize the effect of FFSS on P_{alb}, with or without indomethacin. In the first set of experiments, the effect of the duration of FFSS on the glomerular filtration barrier was determined. Results show that FFSS application for 60 or 120 min resulted in increased P_{alb} ($P < 0.001$). There was no change in P_{alb} in untreated control (T_0) and time-matched (T_{final}) controls (Table 2). In the second set of experiments, results showed persistently elevated P_{alb} at 2 h after (post-2hr) FFSS (Fig. 6, Table 2). Figure 6 shows that pretreatment with indomethacin blocked the effect of FFSS on P_{alb}. In the third and fourth sets of experiments, the effect of FFSS for 120 min on glomeruli pretreated with indomethacin and after an additional 120 min (post-2hr) of recovery following FFSS was studied. The FFSS-induced increase in P_{alb} was significantly blocked by indomethacin. The untreated control (T_0) and time-matched controls (T_{final}) showed no change in P_{alb} (Fig. 6).

Unilateral nephrectomy in sv129 mice is associated with glomerular hypertrophy and increased expression of COX-2 and prostanoid receptor EP2.

Male sv129 mice were uninephrectomized by removing the right kidney to induce hyperfiltration in the remnant solitary kidney. The left kidney was harvested 4 wk later. Table 3 shows that uninephrectomy resulted in significant glomerular hypertrophy by 4 wk as indicated by an increase in glomerular area and volume compared with the left kidney from the sham-operated mice (control). Urine albumin excretion was significantly increased in nephrectomized mice (246.8 ± 141.9 mg/g creatinine) compared with sham-operated mice (25.1 ± 11.4 mg/g creatinine, $P = 0.001$). The mean integrated density (average grey value × area) performed using Image J software for DAB staining for COX and EP proteins provides the net protein expression/glomerulus. Immunohistochemistry showed

Table 2. *FFSS alters the filtration barrier within 1 h indicated by increased glomerular albumin permeability*

	P_{alb} at 60 min		P_{alb} at 120 min	
Untreated control (T_0)	0.03 ± 0.07		0.03 ± 0.07	
Time-matched control (T_{final})	0.02 ± 0.06		0.03 ± 0.07	
FFSS	0.63 ± 0.07	$P < 0.001$	0.77 ± 0.06	$P < 0.001$
Time-matched control (T_{final})	0.00 ± 0.07		0.05 ± 0.09	
FFSS+recovery for 120 min	0.87 ± 0.10	$P < 0.001$	0.62 ± 0.06	$P < 0.001$

Values as means ± SD from 20 glomeruli/group; $n = 4$ rats, 5 glomeruli/rat. P_{alb}, albumin permeability. FFSS (0.3 dyne/cm^2) was applied to isolated decapsulated rat glomeruli for 60 and 120 min, and P_{alb} was again determined after an additional 120 min of recovery at 37°C. Untreated baseline and time-matched glomeruli were used as controls. Changes in P_{alb} in rat glomeruli are shown.
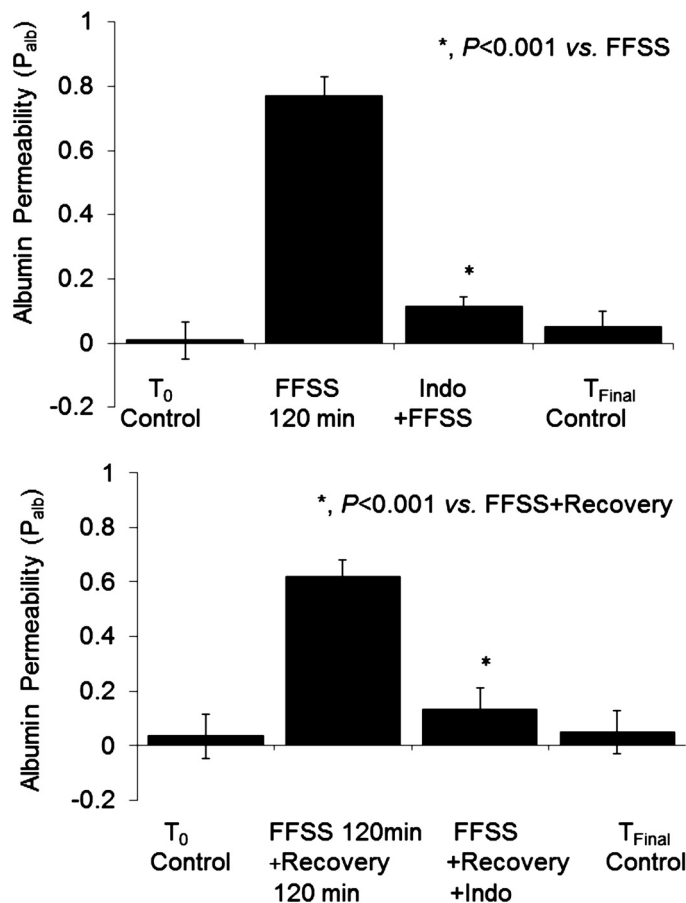
Fig. 6. FFSS application to isolated glomeruli increases albumin permeability (P_{alb}). Isolated rat glomeruli were exposed to FFSS at 0.3 dynes/cm^2 for 120 min with and without pretreatment with indomethacin. Values are means ± SE of P_{alb} determination in 20 glomeruli from 4 rats (5 glomeruli/rat × 4 rats). *Top*: FFSS application for 120 min resulted in increased P_{alb} ($P < 0.001$), while pretreatment with indomethacin blocked the increase in P_{alb}. P_{alb} in untreated control (T_0) and time-matched (T_{final}) controls did not change. *Bottom*: FFSS for 2hr followed by recovery for another 120 min at 37° C showed persistently elevated P_{alb} ($P < 0.001$), while pretreatment with indomethacin blocked the increase in P_{alb}. P_{alb} in untreated control (T_0) and time-matched (T_{final}) controls did not change.

increased mean integrated density for podocyte expression of COX-2 but not COX-1 and prostanoid receptor EP2 but not EP4 (Fig. 7 and Table 4). We also performed a semiquantitative analysis using a 0–4 scale. The mean ± SD on the 0–4 scale for COX-2 staining in the glomeruli for sham and nephrectomy sv129 mice was 1.06 ± 0.40 and 2.45 ± 0.40, respectively ($P = <0.001$), and for COX-1 was 1.29 ± 0.21 and 1.28 ± 0.10, respectively ($P = 0.91$). The mean ± SD integrated density for EP2 staining in the glomeruli for sham and nephrectomy sv129 mice was 0.96 ± 0.34 and 2.45 ± 0.31, respectively ($P = <0.001$) and for EP4 was 3.22 ± 0.34 (sham) vs. 2.83 ± 0.34 (nephrectomy) $P = 0.053$. Thus hyperfiltration resulting from renal mass ablation leads to upregulation of COX-2 and EP2 expression in remnant kidneys of uninephrectomized mice.

DISCUSSION

CAKUT including a solitary kidney is the most common cause of childhood CKD progressing to ESRD. One in 500–1,000 children born with a solitary kidney maintain their total GFR through increased SNGFR and develop adaptive hyperfiltration (34, 51–53). Continued hyperfiltration results in glomerulosclerosis, albuminuria/proteinuria, and progressive azotemia (1, 31, 34, 51–53). The absence of the traditional risk factors of hypertension and proteinuria in early childhood supports the concept that persistent hyperfiltration contributes to kidney injury (34, 52). Additionally, hyperfiltration is an important risk factor in the progression of CKD in adults with diabetes, obesity, and other kidney diseases (1, 8, 20, 31, 50). We believe that hyperfiltration would alter the homeostasis of biomechanical forces that regulates the rheological dynamics within the glomerulus and maintains the filtration barrier.

Glomerular anatomy positions podocytes in Bowman's space, thus exposing these large cells with extensive foot processes to biomechanical forces. Increased intracapillary pressure causes tensile stress on foot processes covering the outer aspect of capillaries, and bulk flow of the filtrate causes FFSS on podocytes (10, 11, 17, 25, 40, 41). A direct measurement of FFSS may be extremely difficult, if not impossible. Mathematical models are heavily relied upon to explore complicated biological problems. We found that the calculated FFSS over podocytes increases 1.5–2-fold in animal models of unilateral nephrectomy (40). We also showed that increased SNGFR, not filtration fraction, is the basis of increased FFSS over podocytes in a solitary kidney. We postulated that hyperfiltration impacts podocyte homeostasis mainly through increased FFSS.

Arachidonic acid metabolites are important mediators of hemodynamic regulation in the kidney. PGE$_2$ is a major product of kidney arachidonic acid metabolism by cyclooxygenases COX-1 and COX-2 (14). As shown in Figs. 2 and 2, COX-2 expression increased as a result of FFSS applied to podocytes, but pretreatment of cells with indomethacin blocked the increase in PGE$_2$ levels and COX-2 expression (Fig. 4 and Table 1). Upregulation of PGE$_2$ synthesis appears to be a specific response to FFSS as neither Martineau et al. (25) nor we (abstract EPAS2008:3803.1) (40a) detected increased PGE$_2$ in podocytes subjected to experimental stretch. A similar increase in COX-2 expression and PGE$_2$ synthesis in renal collecting duct cells was recently demonstrated by Rohatgi and colleagues (15, 23). We did not see a significant change in PGE$_2$ synthesis in control podocytes with no flow and FFSS at 0.2 dynes/cm^2' in contrast to increased PGE$_2$ synthesis and secretion seen with FFSS at 2 dynes/cm^2. Similarly, it has been shown that an increase in PGE$_2$ is seen after a threshold of

Table 3. *Unilateral nephrectomy results in increased glomerular size*

	Sham Mice	Uninephrectomy Mice	P Value
Mean G$_D$, μm	65.6 ± 2.8	72.2 ± 5.0	0.010
Maximum G$_D$, μm	75.4 ± 4.2	82.3 ± 5.2	0.019
Glomerular area, μm^2	3.6 ± 0.3 x 10^3	4.4 ± 0.6 x 10^3	0.006
Glomerular volume, μm^3	297.5 ± 31.1 x 10^3	393.4 ± 74.3 x 10^3	0.008

Values are means ± SD; $n = 7$/group. A solitary kidney was harvested at 4 wk after unilateral nephrectomy of male sv129 mice. Sham-operated mice were used as a control. Morphometric data of measured mean and maximum glomerular diameter (G$_D$) are shown along with calculated glomerular area and glomerular volume.
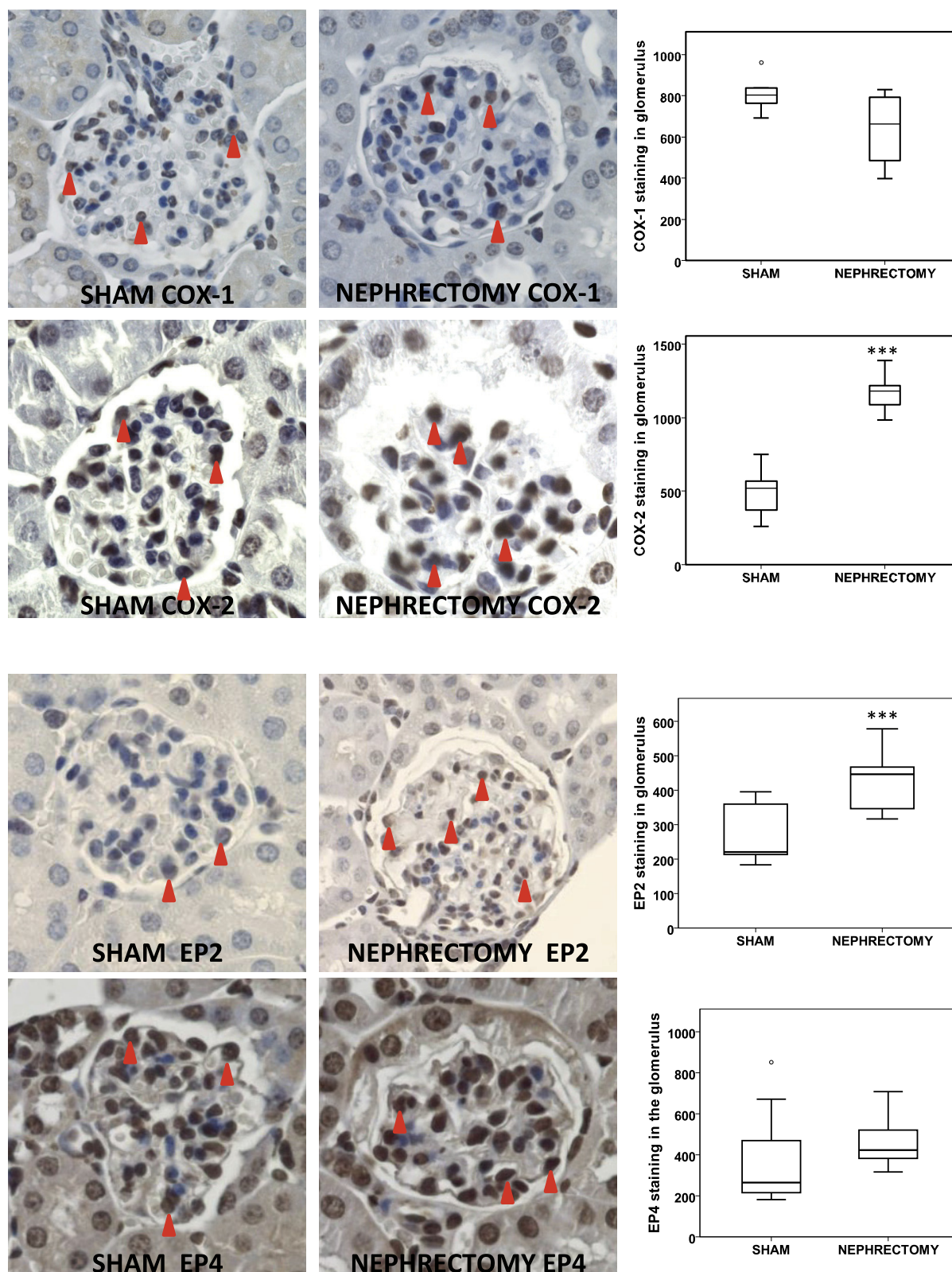
Fig. 7. Unilateral nephrectomy of sv129 mice results in increased glomerular COX-2 and EP2 expression. Hyperfiltration was induced in male sv129 mice by removing the right kidney. The left kidney was harvested 4 wk later. Renal cortical slices were processed for immunohistochemistry using specific antibodies. COX-1, COX-2, EP2, and EP4 expression in podocytes was determined using light microscopy and image analysis. In each glomerulus, a few representative podocytes are marked that show intense immunostaining for the COX and EP proteins. The difference in intensity is shown in the adjoining box plot. Images were observed and analyzed in a masked manner. *Top* 2 rows: light microscopy images of glomerular COX-1 and COX-2 (*left*) with corresponding box plots (*right*). Increased FFSS after unilateral nephrectomy resulted in increased COX-2 expression (*P* = <0.001). *Bottom* 2 rows: light microscopy images of glomerular EP2 and EP4 (*left*) with corresponding box plots (*right*). Increased FFSS after unilateral nephrectomy resulted in increased EP2 expression (*P* = 0.039). °Outlier. ***$P < 0.05$.

Table 4. *Unilateral nephrectomy results in increased glomerular COX-2 and EP2 protein expression*

	Sham Mice	Uninephrectomy Mice	P Value
COX-1	$810.7 \pm 90.1 \times 10^3$	$638.7 \pm 136.3 \times 10^3$	0.07
COX-2	$498.5 \pm 171.4 \times 10^3$	$1,174.5 \pm 136.3 \times 10^3$	<0.001
EP2	$274.5 \pm 95.9 \times 10^3$	$431.0 \pm 46.6 \times 10^3$	0.039
EP4	$381.1 \pm 266.8 \times 10^3$	$464.9 \pm 133.7 \times 10^3$	0.47

Values are means $\pm$ SD for cyclooxygenase (COX)-1, COX-2, EP2, and EP4 staining in 20 consecutive glomeruli in the kidney sections from nephrectomized mice and sham-treated control mice. Solitary kidney was harvested at 4 wk after unilateral nephrectomy of male sv129 mice. Immunohistochemical analysis of COX-1, COX-2, EP2, and EP4 proteins for mean integrated density by Image J analysis is shown. COX-2 protein and EP2 protein were increased following unilateral nephrectomy.

Table 5. *Primer sequences used for qRT-PCR*

Target	PCR Product Size		Sequence
COX-1	70 bp	Forward	5′-CCTCTTTCCAGGAGCTCACA-3′
		Reverse	5′-TCGATGTCACCGTACAGCTC-3′
COX-2	75 bp	Forward	5′-GATGCTCTTCCGAGCTGTG-3′
		Reverse	5′-GGATTGGAACAGCAAGGATTT-3′
EP2	73 bp	Forward	5′-TGCTCCTTGCCTTTCACAAT-3′
		Reverse	5′-CTCGGAGGTCCCACTTTTC-3′
EP4	92 bp	Forward	5′-CGGTTCCGAGACAGCAAA-3′
		Reverse	5′-CGGTTCGATCTAGGAATGG-3′
β-Actin	104 bp	Forward	5′-CTAAGGCCAACCGTGAAAAG-3′
		Reverse	5′-ACCAGAGGCATACAGGGACA-3′

shear stress is reached in renal collecting duct cells (3, 24). These observations also validate the use of cells with no flow as an adequate although not perfect control for in vitro experiments. A continuous treatment with low FFSS is not feasible at the present time due to methodological limitations. Results from in vivo studies also support these findings. For example, in the classic ⅚ nephrectomy rat model, hyperfiltration-mediated injury results in increased PGE$_2$ synthesis and COX-2 expression (30, 43, 49). Since the ⅚ nephrectomy model is confounded by uremia, we preferred the unilateral nephrectomy model to induce hyperfiltration. The unilateral nephrectomy resulted in increased glomerular COX-2 expression in sv129 mice (Fig. 7). Additionally, several studies have shown that chronic inhibition of COX attenuates the progression of kidney injury in animal models and human disease (45–48). Collectively, these findings from in vitro and in vivo studies support our hypothesis that increased FFSS in hyperfiltration induces COX-2 and increases PGE$_2$ levels.

Previously, we reported that FFSS or PGE$_2$ induced a decrease in transversal F-actin stress filaments and the formation of a cortical actin network in podocytes (41). Hyperfiltration-mediated injury is associated with albuminuria/proteinuria, implying glomerular dysfunction. Therefore, we surmised that FFSS-induced changes in the podocyte cytoskeleton would undermine the integrity of the filtration barrier, leading to increased P_{alb}. We have studied the effect of a variety of agents and conditions on the filtration barrier using an in vitro assay of glomerular P_{alb} developed in our laboratory (see METHODS). Our results demonstrate that an increase in P_{alb} precedes the onset of proteinuria in animal models of diabetes, hypertension, radiation nephropathy, puromycin-induced nephrosis, and

focal segmental glomerulosclerosis (9, 33, 36, 39). We have reported that a dose-dependent increase in P_{alb} induced by exogenous PGE$_2$ can be blocked by indomethacin (26, 37). Presently, we designed and constructed a special apparatus for applying FFSS to isolated decapsulated rat glomeruli. Podocytes on the outer aspect of the glomerular tuft would experience similar FFSS as the height, width, and rate of fluid flow are kept constant over the decapsulated glomeruli, but we cannot predict the FFSS that would be experienced by the podocytes present in the inner aspect of the glomerular tuft. Glomeruli exposed to FFSS in this device showed increased P_{alb} at 2 h post-FFSS that was blocked by indomethacin (Table 2 and Fig. 6). In clinical practice, NSAIDs are used occasionally to control proteinuria (45, 46). Vriesendorp et al. (46, 47) found that indomethacin, diclofenac-sodium, or flurbiprofen, NSAIDs that attenuate PGE$_2$ synthesis, also decreased proteinuria. In contrast, sulindac, which does not influence PGE$_2$ synthesis, showed no effect on protein excretion. Thus PGE$_2$ appears to significantly modulate glomerular filtration barrier permselectivity. These results corroborate and complement our findings, suggesting a role for COX-2 and PGE$_2$ in the mechanism of FFSS-induced injury leading to albuminuria/proteinuria.

PGE$_2$ interacts with G protein-coupled receptors (GPCR), of which four (EP$_1$–EP$_4$) have been characterized and cloned (2, 29). EP2, when present, is a low-abundance receptor and believed to be inducible (2, 28, 29). We found that only EP1, EP2, and EP4 are expressed in podocytes and that FFSS did not affect EP1 or induce EP3 gene expression (42). In this study, we focused on EP2 and EP4 because these receptors are upregulated by FFSS (42) and stretch, respectively (12, 13, 25, 44). As shown in Figs. 2 and 5, FFSS upregulated the gene and
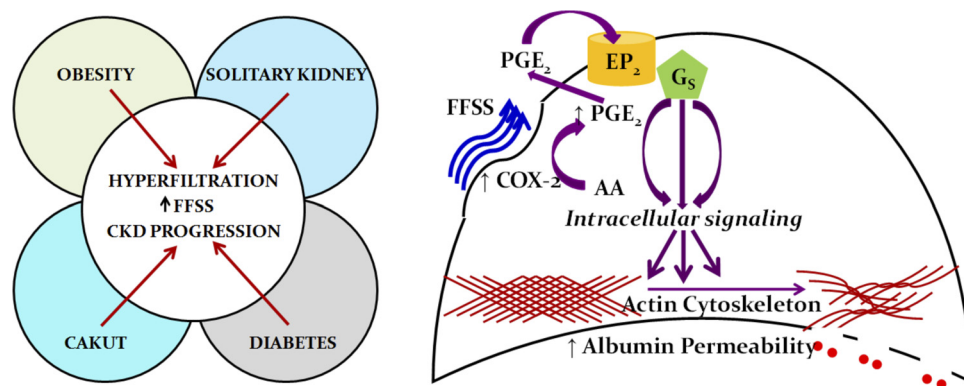

Fig. 8. Schematic summary of working hypothesis. *Left*: several pathophysiological conditions associated with progressive chronic kidney disease (CKD) may share hyperfiltration as a common underlying mechanism. Increased FFSS observed with hyperfiltration is responsible in part for the progression of CKD in conditions such as congenital anomalies of the kidney and urinary tract (CAKUT), a solitary kidney, obesity, and diabetes. *Right*: summary of current working hypothesis that FFSS alters podocyte structure and the actin cytoskeleton via the COX-2-PGE$_2$-EP2 axis and its downstream signaling in pathophysiological conditions associated with hyperfiltration.

protein expression of only EP2 and not EP4 in podocytes. Also, unilateral nephrectomy resulted in the upregulation of glomerular EP2 but not EP4 in sv129 mice (Fig. 7). We have also shown that EP2 is upregulated in mice with low nephron number. Mice with the gene for oligosyndactylism (Os/+) are used as a model to study the effect of congenital deficiency in nephron number. The Os/+ mice are born with ~50% fewer nephrons and have increased SNGFR compared with their wild-type controls (42). Thus in vitro and in vivo studies using podocytes suggest a role for the EP2 receptor in hyperfiltration-induced injury.

EP2 and EP4 are membrane-localized GPCRs that share 30% homology and activate adenylate cyclase. However, these receptors differ with regard to their response to stimuli, nature of ligands, and regulatory mechanisms. For example, resting peritoneal macrophages C3H/HeN express only EP4. While stimulation of these cells by LPS alone induces EP2 and downregulates EP4 expression (18, 19), LPS with indomethacin upregulates EP4. Additionally, EP2 and EP4 respond differently to various ligands. For example, in Chinese hamster ovary (CHO) cells, PGE$_2$ causes only short-term desensitization of EP4 without affecting EP2, and 15-keto-PGE$_2$ causes an immediate reduction in EP4 activity and a gradual but greater loss of EP2 activity (32). Thus the increase in EP4 gene expression by indomethacin observed in our experiments (Fig. 2) is intriguing and unexplained but not surprising.

Studies on EP receptors in osteocytes serve as a very supportive parallel example for our observations (6, 7, 16, 21). Osteocytes located within the bone canaliculi form a network of cytoplasmic processes and respond to tensile and shear stress (27). Both osteocytes and podocytes are terminally differentiated cells that possess elaborate cytoplasmic extensions and respond to FFSS (6, 7, 16, 21, 41, 42). A head-to-head comparison of shear and tensile forces in osteocytes shows that FFSS induces greater cellular deformity (27) and upregulates COX-2 (6, 7, 16, 21). Furthermore, FFSS upregulates EP2 in osteocytes without altering EP4 expression (6, 7, 16, 21). These studies have been useful in comprehending the role of biomechanical forces in diverse cell types.

A comparison of mechanical forces shows that tensile stress 1) causes formation of actin-rich centers and radial stress fibers, 2) upregulates COX-2 without increasing PGE$_2$ synthesis, and 3) upregulates EP4 but not EP2 in podocyte cultures (12, 13, 25, 44). In contrast, FFSS 1) disrupts actin stress fibers with the formation of a cortical actin ring, 2) upregulates COX-2 with increased PGE$_2$ levels, and 3) upregulates EP2 but not EP4 in cultured podocytes (17, 41, 42). Based on these considerations, we have developed a model (Fig. 8; see the legend) to study the role of FFSS in hyperfiltration-mediated injury in the progression of CKD. Although in vitro studies can dissect the subtle differences between FFSS and stretch, these forces are likely to exert their influence concurrently in vivo. Future studies using specific receptor agonists/antagonists, an idealized control, and animal models will further strengthen our observations and delineate the cellular signaling events.

In summary, similarities in the effects of FFSS on podocytes, osteocytes, and recently reported results on renal colleting duct cells suggest a conserved cellular response involving the COX2-PGE$_2$-EP2 axis that warrants additional investigation for its role in hyperfiltration-mediated kidney injury. We believe the COX2-PGE$_2$-EP2 axis is a potential target for developing new interventions to prevent CKD progression.

DISCLOSURES

No conflicts of interest, financial or otherwise, are declared by the authors.

AUTHOR CONTRIBUTIONS

Author contributions: T.S., U.S.A., E.T.M., R.S., M.L.J., L.F.B., A.E.-M., V.J.S., and M.S. provided conception and design of research; T.S., P.A.C., R.S.D., M.L.J., and M.S. performed experiments; T.S., P.A.C., B.T., A.K., R.E.G., R.S.D., R.S., and M.S. analyzed data; T.S., U.S.A., A.K., R.E.G., E.T.M., R.S., M.L.J., L.F.B., A.E.-M., V.J.S., and M.S. interpreted results of experiments; T.S., A.K., and M.S. prepared figures; T.S. and M.S. drafted manuscript; T.S., U.S.A., P.A.C., A.K., R.E.G., R.S.D., E.T.M., R.S., M.L.J., L.F.B., A.E.-M., V.J.S., and M.S. edited and revised manuscript; T.S., U.S.A., P.A.C., B.T., A.K., R.E.G., R.S.D., E.T.M., R.S., M.L.J., L.F.B., A.E.-M., V.J.S., and M.S. approved final version of manuscript.

REFERENCES

1. **Brenner BM, Mackenzie HS.** Nephron mass as a risk factor for progression of renal disease. *Kidney Int Suppl* 63: S124–S127, 1997.
2. **Breyer MD, Davis L, Jacobson HR, Breyer RM.** Differential localization of prostaglandin E receptor subtypes in human kidney. *Am J Physiol Renal Fluid Electrolyte Physiol* 270: F912–F918, 1996.
3. **Carrisoza-Gaytan R, Liu Y, Flores D, Else C, Lee HG, Rhodes G, Sandoval RM, Kleyman TR, Lee FY, Molitoris B, Satlin LM, Rohatgi R.** Effects of biomechanical forces on signaling in the cortical collecting duct (CCD). *Am J Physiol Renal Physiol* 307: F195–F204, 2014.
4. **Celsi G, Larsson L, Seri I, Savin V, Aperia A.** Glomerular adaptation in uninephrectomized young rats. *Pediatr Nephrol* 3: 280–285, 1989.
5. **Celsi G, Savin J, Henter Jl Sohtell M.** The contribution of ultrafiltration pressure for glomerular hyperfiltration in young nephrectomized rats. *Acta Physiol Scand* 141: 483–487, 1991.
6. **Cheng B, Kato Y, Zhao S, Luo J, Sprague E, Bonewald LF, Jiang JX.** PGE$_2$ is essential for gap junction-mediated intercellular communication between osteocyte-like MLO-Y4 cells in response to mechanical strain. *Endocrinology* 142: 3464–3473, 2001.
7. **Cherian PP, Cheng B, Gu S, Sprague E, Bonewald LF, Jiang JX.** Effects of mechanical strain on the function of gap junctions in osteocytes are mediated through the prostaglandin EP2 receptor. *J Biol Chem* 278: 43146–43156, 2003.
8. **Christinasen JS, Gammelgaard J, Frandsen M, Parving HH.** Increased kidney size, glomerular filtration rate and renal plasma flow in short-term insulin-dependent diabetics. *Diabetlogia* 20: 451–456, 1981.
9. **Dahly-Vernon AJ, Sharma M, McCarthy ET, Savin VJ, Ledbetter SR, Roman RJ.** Transforming growth factor-α, 20-HETE interaction, and glomerular injury in Dahl salt-sensitive rats. *Hypertension* 45: 1–6, 2005.
10. **Durvasula RV, Petermann AT, Hiromura K, Blonski M, Pippin J, Mundel P, Pichler R, Griffin S, Couser WG, Shankland SJ.** Activation of a local tissue angiotensin system in podocytes by mechanical strain. *Kidney Int* 65: 30–39, 2004.
11. **Endlich N, Kress KR, Reiser J, Uttenweiler D, Kriz W, Mundel P, Endlich K.** Podocytes respond to mechanical stress in vitro. *J Am Soc Nephrol* 12: 413–422, 2001.
12. **Faour WH, Gomi K, Kennedy CR.** PGE$_2$ induces COX-2 expression in podocytes via the EP4 receptor through a PKA-independent mechanism. *Cell Signal* 20: 2156–2164, 2008.
13. **Faour WH, Thibodeau JF, Kennedy CR.** Mechanical stretch and prostaglandin E2 modulate critical signaling pathways in mouse podocytes. *Cell Signal* 22: 1222–1230, 2010.
14. **FitzGerald GA.** The choreography of cyclooxygenases in the kidney. *J Clin Invest* 110: 33–34, 2002.
15. **Flores D, Liu Y, Liu W, Satlin LM, Rohatgi R.** Flow-induced prostaglandin E$_2$ release regulates Na and K transport in the collecting duct. *Am J Physiol Renal Physiol* 303: F632–F638, 2012.

16. **Forwood MR.** Inducible cyclo-oxygenase (COX-2) mediates the induction of bone formation by mechanical loading in vivo. *J Bone Miner Res* 11: 1688–1693, 1996.

17. **Friedrich C, Endlich N, Kriz W, Endlich K.** Podocytes are sensitive to fluid shear stress in vitro. *Am J Physiol Renal Physiol* 291: F856–F865, 2006.

18. **Ikegami R, Sugimoto Y, Segi E, Katsuyama M, Karahashi H, Amano F, Maruyama T, Yamane H, Tsuchiya S, Ichikawa A.** The expression of prostaglandin E receptors EP2 and EP4 and their different regulation by lipopolysaccharide in C3H/HeN peritoneal macrophages. *J Immunol* 166: 4689–4696, 2001.

19. **Katsuyama M, Ikegami R, Karahashi H, Amano F, Sugimoto Y, Ichikawa A.** Characterization of the LPS-stimulated expression of EP2 and EP4 prostaglandin E receptors in mouse macrophage-like cell line, J774.1 *Biochem Biophys Res Commun* 251: 727–731, 1998.

20. **Keller G, Zimmer G, Mall G, Ritz E, Amann K.** Nephron number in patients with primary hypertension. *N Engl J Med 348*: 101–108, 2003.

21. **Kitase Y, Barragan L, Qing H, Kondoh S, Jiang JX, Johnson ML, Bonewald LF.** Mechanical induction of PGE2 in osteocytes blocks glucocorticoid-induced apoptosis through both the β-catenin and PKA pathways. *J Bone Miner Res* 25: 2657–2668, 2010.

22. **Kömhoff M, Grone HJ, Klein T, Seyberth HW, Nüsing RM.** Localization of cyclooxygenase- 1 and -2 in adult and fetal human kidney: implication for renal function. *Am J Physiol Renal Physiol* 272: F460–F468, 1997.

23. **Liu Y, Flores D, Carrisoza-Gaytan R, Rohatgi R.** Biomechanical regulation of cyclooxygenase-2 in the renal collecting duct. *Am J Physiol Renal Physiol* 306: F214–F223, 2014.

24. **Liu W, Xu S, Woda C, Kim P, Weinbaum S, Satlin LM.** Effect of flow and stretch on the $(Ca^{2+})_i$ response of principal and intercalated cells in cortical collecting duct. *Am J Physiol Renal Physiol* 285: F998–F1012, 2003.

25. **Martineau LC, McVeigh LI, Jasmin BJ, Kennedy CR.** p38 MAP kinase mediates mechanically induced COX-2 and PG EP4 receptor expression in podocytes: implications for the actin cytoskeleton. *Am J Physiol Renal Physiol* 286: F693–F701, 2004.

26. **McCarthy ET, Sharma M.** Indomethacin protects permeability barrier from focal segmental glomerulosclerosis serum. *Kidney Int* 61: 534–541, 2002.

27. **McGarry JG, Klein-Nulend J, Mullender MG, Prendergast PJ.** A comparison of strain and fluid shear stress in stimulating bone cell responses-a computational and experimental study. *FASEB J* 19: 482–484, 2005.

28. **Morath R, Klein T, Seyberth HW, Nusing RM.** Immunolocalization of the four prostaglandin E-2 receptor proteins EP1, EP2, EP3, and EP4 in human kidney. *J Am Soc Nephrol* 10: 1851–1860, 1999.

29. **Narumiya S, Sugimoto Y, Ushikubi F.** Prostanoid receptors: structures, properties, functions. *Physiol Rev* 79: 1193–1226, 1999.

30. **Nath KA, Chmielewski DH, Hostetter TH.** Regulatory role of prostanoids in glomerular microcirculation of remnant nephrons. *Am J Physiol Renal Fluid Electrolyte Physiol* 252: F829–F837, 1987.

31. **Neuringer JR, Brenner BM.** Hemodynamic theory of progressive renal disease: a 10-year update in brief review. *Am J Kidney Dis* 22: 98–104, 1993.

32. **Nishigaki N, Negishi M, Ichikawa A.** Two Gs-coupled prostaglandin E receptor subtypes, EP2 and EP4, differ in desensitization and sensitivity to the metabolic inactivation of the agonist. *Mol Pharmacol* 50: 1031–1037, 1996.

33. **Rangel-Filho A, Sharma M, Datta Y, Moreno C, Roman RJ, Iwamoto Y, Provoost A, Lazar J, Jacob HJ.** Rab38 is the RF-2 gene and it modulates proteinuria and albuminuria independently of changes in glomerular permeability in the Fawn Hooded hypertensive rat. *J Am Soc Nephrol* 16: 852–856, 2005.

34. **Sanna-Cherci S, Ravani P, Corbani V, Parodi S, Haupt R, Piaggio G, Innocenti ML, Somenzi D, Trivelli A, Caridi G, Izzi C, Scolari F, Mattioli G, Allegri L, Ghiggeri GM.** Renal outcome in patients with congenital anomalies of the kidney and urinary tract. *Kidney Int* 76: 528–533, 2009.

35. **Savin VJ, Sharma R, Lovell HB, Weilling DJ.** Measurement of albumin reflection coefficient with isolated rat glomeruli. *J Am Soc Nephrol* 3: 1260–1269, 1992.

36. **Savin VJ, Sharma R, Sharma M, McCarthy ET, Swan SK, Ellis E, Lovell H, Warady B, Gunwar S, Chonko AM, Artero M, Vincenti F.** Circulating factor associated with increased glomerular permeability to albumin in recurrent focal segmental glomerulosclerosis. *N Engl J Med* 334: 878–883, 1996.

37. **Sharma M, McCarthy ET, Sharma R, Fish BL, Savin VJ, Cohen EP, Moulder JE.** Arachidonic acid metabolites mediate the radiation-induced increase in glomerular albumin permeability. *Exp Biol Med* 231: 99–106, 2006.

38. **Sharma M, Sharma R, McCarthy ET, Savin VJ.** The focal segmental glomerulosclerosis permeability factor: biochemical characteristics and biological effects. *Exp Biol Med* 229: 85–98, 2004.

39. **Sharma R, Sharma M, Reddy S, Savin VJ, Nagaria AM, Wiegmann TB.** Chronically increased intrarenal angiotensin II causes nephropathy in an animal model of type 2 diabetes. *Front Biosci* 1: 968–976, 2006.

40. **Srivastava T, Celsi GE, Sharma M, Dai H, McCarthy ET, Ruiz M, Cudmore PA, Alon US, Sharma R, Savin VJ.** Fluid flow shear stress over podocytes is increased in the solitary kidney. *Nephrol Dial Transplant* 1: 65–72, 2014.

40a.**Srivastava T, Cudmore PA, Sharma R, Carlton C, McCarthy ET.** Fluid flow shear stress (FF) but not substrate stretch (SS) increases podocyte release of prostaglandin E$_2$ (PGE$_2$). EPAS2008:3803.1.

41. **Srivastava T, McCarthy ET, Sharma R, Cudmore PA, Sharma M, Johnson ML, Bonewald LF.** Prostaglandin E2 is crucial in the response of podocytes to fluid flow shear stress. *J Cell Commun Signal* 4: 79–90, 2010.

42. **Srivastava T, McCarthy ET, Sharma R, Kats A, Carlton CG, Alon US, Cudmore PA, El-Meanawy A, Sharma M.** Fluid flow shear stress upregulates prostanoid receptor EP2, but not EP4 in murine podocytes. *Prostaglandins Other Lipid Mediat* 104–105: 49–57, 2013.

43. **Stahl RA, Kudelka S, Paravicini M, Schollmeyer P.** Prostaglandin and thromboxane formation in glomeruli from rats with reduced renal mass. *Nephron* 42: 252–257, 1986.

44. **Stitt-Cavanagh EM, Faour WH, Takami K, Carter A, Vanderhyden B, Guan Y, Schneider A, Breyer MD, Kennedy CRJ.** A maladaptive role for EP4 receptors in podocytes. *J Am Soc Nephrol* 21: 1678–1690, 2010.

45. **Velosa JA, Torres VE, Donadio JV Jr, Wagoner RD, Holley KE, Offord KP.** Treatment of severe nephritic syndrome with meclofenamate: an uncontrolled pilot study. *Mayo Clin Proc* 60: 586–592, 1985.

46. **Vriesendorp R, de Zeeuw D, de Jong PE, Donker AJ, Pratt JJ, van der Hem GK.** Reduction of urinary protein and prostaglandin E2 excretion in the nephritic syndrome by non-steroidal anti-inflammatory drugs. *Clin Nephrol* 25: 105–110, 1986.

47. **Vriesendorp R, Donker AJ, de Zeeuw D, de Jong PE, van der Hem GK, Brentjens JR.** Effects of nonsteroidal anti-inflammatory drugs on proteinuria. *Am J Med* 81: 84–94, 1986.

48. **Wang JL, Cheng HF, Shappell S, Harris RC.** A selective cyclooxygenase-2 inhibitor decreases proteinuria and retards progressive renal injury in rats. *Kidney Int* 57: 2334–2342, 2000.

49. **Wang JL, Cheng HF, Zhang MZ, McKanna JA, Harris RC.** Selective increase of cyclooxygenase-2 expression in a model of renal ablation. *Am J Physiol Renal Physiol* 275: F613–F622, 1998.

50. **Wang JT, Evans JC, Meigs JB, Rifai N, Fox CS, D'Agostino RB, Levy D, Vasan RS.** Low-grade albuminuria and the risks of hypertension and blood pressure progression. *Circulation* 111: 1370–1376, 2005.

51. **Westland R, Kurvers RA, van Wijk JA, Schreuder MF.** Risk factors for renal injury in children with a solitary functioning kidney. *Pediatrics* 131: e478–e485, 2013.

52. **Westland R, Schreuder MF, Bökenkamp A, Spreeuwenberg MD, Van WiJk JA.** Renal injury in children with a solitary functioning kidney-the KIMONO study. *Nephrol Dial Transplant* 26: 1533–1541, 2011.

53. **Westland R, Schreuder MF, Ket JC, van Wijk JA.** Unilateral renal agenesis: a systematic review on associated anomalies and renal injury. *Nephrol Dial Transplant* 28: 1844–1855, 2013.